

Initial Experiments with a Flexible Robot

Andrew D. Christian and Warren P. Seering

Department of Mechanical Engineering
Massachusetts Institute of Technology
Cambridge, MA 02139

Abstract

This paper describes a flexible three degree of freedom robot and compares its behavior with a simple model of a vibrating system. The robot has three rotary joints and two flexible steel links, causing it to exhibit many complicated modes of vibration. We present a non-dimensional analysis of the model showing how it responds to ramp commands and acceleration commands, and then compare these with the actual robot. Using the model we can select input commands that minimize the vibration of the robot.

Introduction

Many research groups over the last decade have built flexible test fixtures to experiment with methods of controlling systems that vibrate. These test fixtures come in a variety of configurations: simple single degree of freedom beams [1, 3], planar two degree of freedom arms [2, 4, 8, 10], and complete three degree of freedom robots [7, 9]. We have constructed a system which falls into the final category. It has two links, three joints, and exhibits both link and joint flexibility (see [5, 6]). We have nicknamed it the "Flexbot", and it will be described in greater detail later in this paper.

Before we began trying complicated control strategies on the Flexbot, we decided to see how well we could control vibration with an ordinary PD servo loop and simple step, ramp, and acceleration inputs. We used a simple model of the robot to predict the robot's behavior and then verified the model experimentally. These experiments serve two purposes: First, they form a baseline to which future control strategies can be compared. Second, in many cases implementing a complicated controller is not practical or a robot is already controlled with a PD servo loop; hence it is useful to see how much vibration can be eliminated by careful choice of speeds and accelerations.

The paper is broken up into the following sections: an explanation of the model, a description of the test fixture, and a comparison between the model and experimental results.

Model

A well constructed, complex model of a dynamic system can accurately predict how a dynamic system will behave.

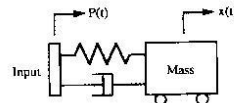


Figure 1: Theoretical Model

Such a model leads to a greater understanding of the system and how to improve performance. Unfortunately, a complicated model rarely applies to more than one dynamic system. Our model is deliberately simple so that it can apply to virtually any system.

This section of the paper presents the theoretical behavior of a simple model responding to several common types of input. The model is shown in figure 1; it consists of a mass/spring/damper connected to a plate whose position $P(t)$ is specified as a function of time. We chose this model for three reasons: First, by non-dimensionalization its response to a family of inputs can be captured by a few graphs. Second, this type of model is often used in dynamic analysis and is well understood. Third, this particular model is a good approximation to the general behavior of a system that has a distinct first mode of vibration.

For the purposes of this paper we will compare input functions based on the amplitude of residual vibration in the system after the commanded input is over. We will assume that the system is underdamped.

With initial conditions given, the free response of a second order underdamped system can be written as

$$x(t) = e^{-\zeta\omega_n t} \left(\frac{v_0 + \zeta\omega_n x_0}{\omega_d} \sin \omega_d t + x_0 \cos \omega_d t \right) \quad (1)$$

where ζ is the damping ratio, $\omega_n/2\pi$ is the undamped natural frequency of vibration, $\omega_d/2\pi$ is the damped natural frequency of vibration, x_0 is the initial position, and v_0 is the initial velocity.

Equation 1 can be written as $Ae^{-\zeta\omega_n t} \sin(\omega_d t + \phi)$, where A is the amplitude of vibration and ϕ is a phase offset. We can calculate the non-dimensionalized amplitude

with respect to the commanded move distance as

$$\frac{A}{D} = \left[\left(\frac{x_0}{D} \right)^2 + \left(\frac{v_0}{D\omega_d} + \frac{\zeta}{\sqrt{1-\zeta^2}} \frac{x_0}{D} \right)^2 \right]^{1/2} \quad (2)$$

where D is the commanded move distance. To compare our different input functions, we will calculate the value of A/D at the instant the command finishes and call this the (non-dimensionalized) amplitude of residual vibration.

The simplest input to the model is a step input. This gives a damped oscillation with an amplitude of

$$\frac{A}{D} = \sqrt{\frac{1+\zeta^2}{1-\zeta^2}} \quad (3)$$

For the step input, the non-dimensionalized amplitude is always greater than or equal to one. If minimizing residual vibration in a system is important, step inputs are bad.

Response to a Ramp Input

The step input is the limiting case of a ramp input, where the commanded position changes at a constant velocity. A standard ramp input $P(t)$ in position is of the form

$$P(t) = \begin{cases} Vt & 0 \leq t < t_f \\ Vt_f & t \geq t_f \end{cases} \quad (4)$$

where t_f is the time required to complete the move and V is the velocity of the move.

The model response to a simple ramp input $P(t) = Vt$ starting at $t = 0$ is

$$x(t) = V \left[t - \frac{1}{\omega_d} e^{-\zeta\omega_n t} \sin \omega_d t \right] \quad (5)$$

$$\dot{x}(t) = V \left[1 + e^{-\zeta\omega_n t} \left(\frac{\zeta}{\sqrt{1-\zeta^2}} \sin \omega_d t - \cos \omega_d t \right) \right] \quad (6)$$

To find the response for the general ramp input, we superpose two simple ramp inputs and solve for the non-dimensionalized error in position X_f and velocity V_f at time t_f . Given that $D = Vt_f$, we can write X_f and V_f as

$$\frac{X_f}{D} = 1 - \frac{1}{2\pi(t_f/\tau)} \exp\left(\frac{-2\pi\zeta}{\sqrt{1-\zeta^2}} \frac{t_f}{\tau}\right) \sin \frac{2\pi t_f}{\tau} \quad (7)$$

$$\frac{V_f}{D\omega_d} = \frac{1}{2\pi(t_f/\tau)} \left[1 + \exp\left(\frac{-2\pi\zeta}{\sqrt{1-\zeta^2}} \frac{t_f}{\tau}\right) \left(\frac{\zeta}{\sqrt{1-\zeta^2}} \sin \frac{2\pi t_f}{\tau} - \cos \frac{2\pi t_f}{\tau} \right) \right] \quad (8)$$

where $\tau = 2\pi/\omega_d$, the time constant of the system.

Equations (7) and (8) combined with equation (2) yield the nondimensional amplitude of the residual vibration as a function of t_f/τ and ζ . This curve is plotted in figure 2 for a variety of values of ζ .

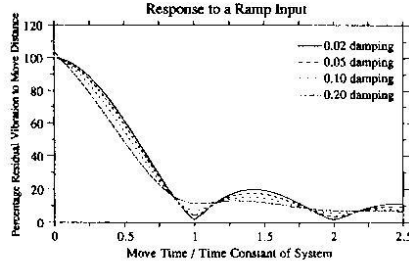


Figure 2: Nondimensionalized response of the model to a ramp input

An interesting result from figure 2 is that for low damping ratios there are move times that result in almost no residual vibration. These times correspond to commanded moves that are an integral number of vibration cycles long.

Acceleration Response

Giving the model a ramp input assumes that it can accelerate infinitely fast. This abrupt application of force induces vibration. In many applications it is better to accelerate up to speed slowly, travel at a constant velocity for a while, and then decelerate to stop.

The response of the model to a simple acceleration input $P(t) = \frac{1}{2}\alpha t^2$ (for $t > 0$) can be found to be

$$x(t) = \frac{\alpha}{\omega_n^2} e^{-\zeta\omega_n t} \left(\frac{\zeta}{\sqrt{1-\zeta^2}} \sin \omega_d t + \cos \omega_d t \right) + \frac{1}{2}\alpha t^2 - \frac{\alpha}{\omega_n^2} \quad (9)$$

$$v(t) = \frac{-\alpha}{\omega_d} e^{-\zeta\omega_n t} \sin \omega_d t + \alpha t \quad (10)$$

To find the response of the system to a general acceleration input we superpose 4 simple acceleration inputs. Define t_a as the time the system spends accelerating up to speed and t_f as the overall move time. Then the input function $P(t)$ can be written as

$$P(t) = \begin{cases} \frac{1}{2}\alpha t^2 & 0 \leq t < t_a \\ \alpha t_a(t - t_a/2) & t_a \leq t < (t_f - t_a) \\ \alpha [t_a(t_f - t_a) - \frac{1}{2}(t_f - t)^2] & (t_f - t_a) \leq t < t_f \\ \alpha t_a(t_f - t_a) & t > t_f \end{cases} \quad (11)$$

To calculate the result of this function, we note that the distance moved $D = \alpha t_a(t_f - t_a)$. We also define $\gamma = 2t_a/t_f$ ($0 < \gamma \leq 1$) which represents the fraction of time the system is accelerating or decelerating. The non-dimensionalized error in position X_f and velocity V_f of the model at time t_f can then be found as

$$\frac{X_f}{D} = \frac{(1-\zeta^2)(\ddot{x}(t_f) - \ddot{x}(t_f - t_a) - \ddot{x}(t_a) + \ddot{x}(0))}{\pi^2\gamma(2-\gamma)(t_f/\tau)^2} \quad (12)$$

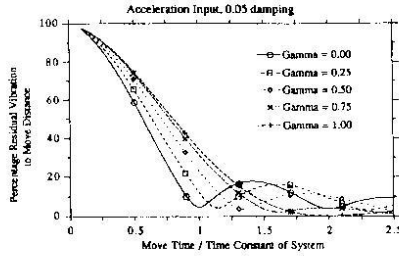


Figure 3: Response of the model to an acceleration input, with 0.05 damping and different values of γ

$$\frac{V_f}{D\omega_d} = \frac{(\ddot{v}(t_f) - \ddot{v}(t_f - t_a) - \ddot{v}(t_a) + \ddot{v}(0))}{\pi^2 \gamma (\gamma - 2)(t_f/\tau)^2} \quad (13)$$

where we define

$$\ddot{x}(t) = \exp\left(\frac{-2\pi\zeta}{\sqrt{1-\zeta^2}} \frac{t}{\tau}\right) \left(\frac{\zeta}{\sqrt{1-\zeta^2}} \sin \frac{2\pi t}{\tau} + \cos \frac{2\pi t}{\tau} \right) \quad (14)$$

$$\ddot{v} = \exp\left(\frac{-2\pi\zeta}{\sqrt{1-\zeta^2}} \frac{t}{\tau}\right) \sin \frac{2\pi t}{\tau} \quad (15)$$

Using these values and equation (2) we can then calculate the amplitude of the residual vibration of the simple model to an acceleration style input. This amplitude is a function of ζ , t_f/τ and γ . Note that as $\gamma \rightarrow 0$ the response approaches the ramp input.

As the amplitude is a function of three variables, there is no convenient way to display the entire range of possibilities on a single graph. Figures 3 and 4 show typical response curves for different damping ratios and values of γ . It can be shown that the minimal amount of residual vibration occurs approximately when the time between the beginning of the acceleration phase and the beginning of the deceleration phase is equal to an integral number of time constants of the system.

Experimental Setup

Figure 5 is a schematic of the MJT Flexbot, a flexible robot designed for experiments in vibration control. The Flexbot has three rotary actuators and two links; two of the actuators are located in the base and the third sits between the links as an elbow joint. The two actuators at the base are DC servo motors connected to 10:1 timing belt reductions. The elbow joint uses a DC torque motor connected to a 5:1 planetary gear set. Position information is read from optical encoders connected to the motor shafts.

To make the robot vibrate at low frequencies we use flexible links and joints. The links are narrow steel rods which are attached with just four bolts at each joint. Variable flexibility is provided at the joints by a stack of spring

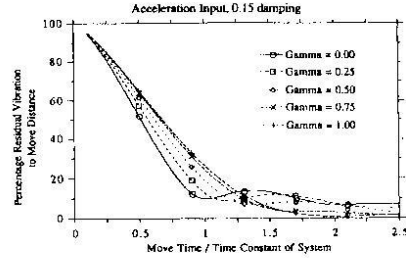


Figure 4: Response of the model to an acceleration input, with 0.15 damping and different values of γ

washers between the gear reduction and the output. The robot carries a 3 pound payload, has a reach of 51 inches, and has a peak acceleration of over 240 ft/sec² at the tip when fully extended.

The robot is controlled by three 68000 based processor boards and a number of interface boards on a VMEbus backplane. A Sun 3/180 workstation running the Condor system provides the development environment and data storage. The current controller is a PD servo loop running at 1000 Hz. A teleoperator box is used for endpoint control of the robot in cartesian space.

Vibrational Characteristics of the Flexbot

For most experiments it is sufficient to consider just the four principle frequencies of vibration of the Flexbot. They can be divided into two categories. Holding the base axis still, picture the plane swept out by the second link when the elbow joint moves. Two of the low vibrational modes lie approximately in this plane ("planar" vibration) and two of the modes are primarily perpendicular to this plane ("out-of-plane" vibration).

To map out the vibrational behavior of the arm we attached an accelerometer to the payload of the robot, positioned it throughout the workspace, and performed a frequency analysis of the response of the arm to an impulse. The impulse was supplied either by an abrupt movement of the robot, or a hammer. Figure 6 is a plot of the natural frequencies obtained for planar vibrations. The position of the base axis does not affect the frequencies. The elbow joint is considered to have a position of 0 degrees when it is fully extended; that is, when the two links lie on the same line.

Out-of-plane vibrations are more complicated because they are a function of the position of both the upper base joint and the elbow joint. Figures 7 and 8 show contour plots of the experimental data obtained. The base joint is considered to be at a position of 0 degrees when it is pointing straight up. The position of the elbow joint is measured relative to the position of the base joint. Damp-

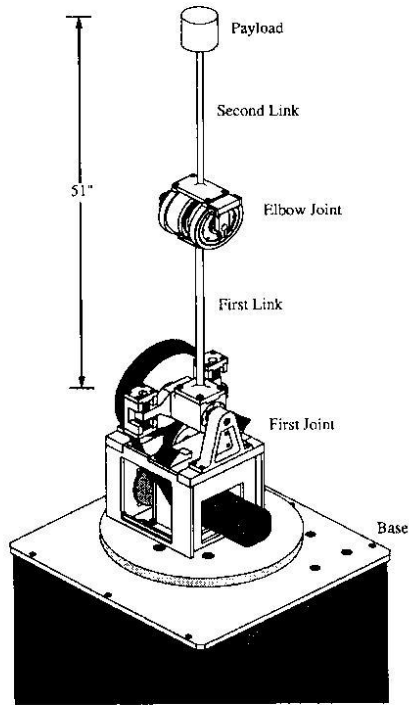


Figure 5: Vibration control test fixture

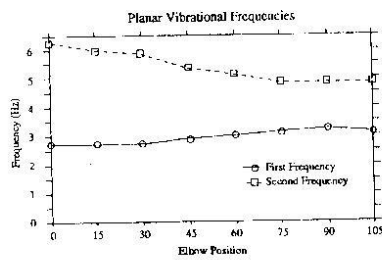


Figure 6: Planar vibrational frequencies

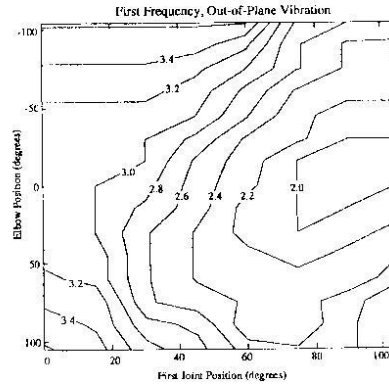


Figure 7: Out-of-plane vibrational frequencies, lowest mode of vibration.

ing ratios range from a low of $\zeta < 0.01$ for out-of-plane vibrations with the arm pointing straight up to a high of $\zeta > 0.2$ with the arm fully outstretched and vibrating in the plane.

Experimental Results

The final section of this paper compares the model with the behavior of the Flexbot. For this comparison we chose the motion shown in figure 9; the base of the robot rotates 100 degrees and the other two joints remain fixed. The advantage of this motion is that the vibrational frequencies of the Flexbot do not change during the move. We chose a long move to keep the value of t_f/r larger than 1; shorter motions do not allow enough time to compare different accelerations. The primary mode of vibration excited was the out-of-plane first mode, which has a damped natural frequency of 2.75 hertz, and a 0.10 damping ratio.

Figure 10 is a sample of the data recorded. The command used was a ramp input with a slew rate of 60 deg/sec. The position of the robot is measured by the encoder attached to the base motor. The encoder has a resolution of 0.009 degrees and data was collected at 250 Hertz. The data recorded is the position of the base—not the position of the payload. Since most of the flexibility of the robot is in the links, when the amplitude of the base vibration is one degree the payload is actually vibrating with an amplitude of 5.5 inches.

Measuring the amplitude of the residual vibration from a move proved to be difficult, especially as higher modes of vibration showed up in the faster moves, so instead we compare settling times. We defined the settling time as the time from when the commanded move finished

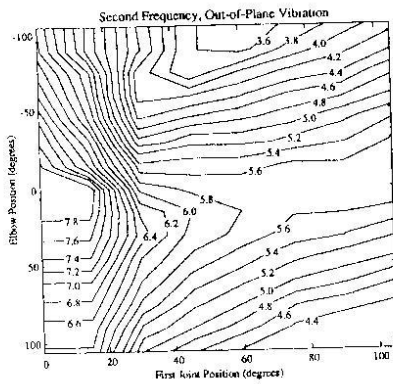


Figure 8: Out-of-plane vibrational frequencies, second mode of vibration

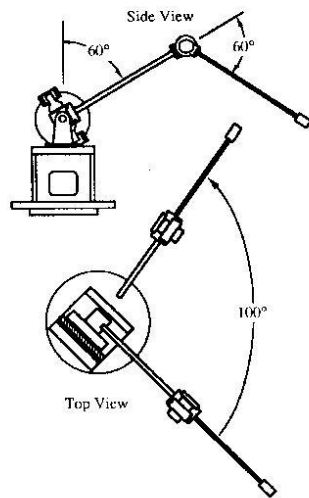


Figure 9: Experimental motion for tests

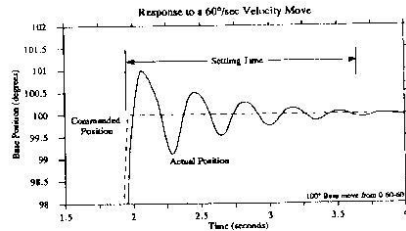


Figure 10: A sample motion of the Flexbot. The position of the base is plotted against time.

to the time the amplitude of base vibration dropped beneath 0.05 degrees. Using the amplitude found by the theoretical model, we can calculate the settling time as

$$t_s = \frac{\tau (\ln(A/S) - \ln 0.05)}{-2\pi\zeta/\sqrt{1-\zeta^2}} \quad (16)$$

where A is the theoretical amplitude, t_s is the calculated settling time, and S is a scaling factor. The scaling factor is necessary because we are not measuring the amplitude of a lumped mass system. The flexibility is partially in the servo and partially in the steel links. Since we are measuring the vibration at a point between these two flexibilities, we have to scale the theoretical amplitude. In this system, $S \approx 4$.

Experimental vs. Theoretical

We illustrate the correlation between theoretical and experimental with three types of sample moves. The first is a ramp input, run at several different slew rates. The second and third are acceleration moves; one slow and one fast.

Figure 11 compares the theoretical response to a ramp input with the experimental response. We did not run the robot at velocities faster than 100 deg/sec because we were afraid it would break.

For the acceleration moves we set the acceleration rate and move distance and then ran the robot at different peak velocities. Hence the value of τ is different for each point on the chart; it is as low as 0.2 for slow velocities and equal to 1.0 for the fastest data point of both the slow and fast acceleration rates. The slow acceleration rate is 100 deg/sec² and the fast acceleration rate is 200 deg/sec². Figure 12 shows the settling times for the different accelerations and velocities.

The experimental results match up fairly well with the model in the case of the ramp input and at lower speeds with the acceleration input. At the higher velocities, the Flexbot tends to settle faster than the model would predict. There are many factors that were not taken into account by the simplistic model that can account for this.

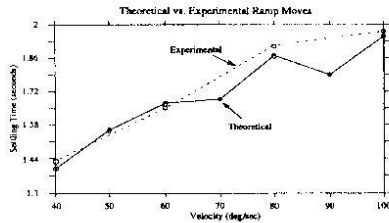


Figure 11: Response of the Flexbot to a ramp input. The solid curve represents the theoretical response, the marks on the dotted line are the measured response.

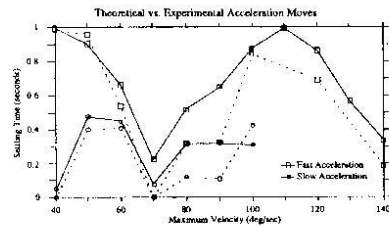


Figure 12: Response of the Flexbot to acceleration input. The solid curves represent the theoretical response, the marks on the dotted lines are the measured response.

The most likely three are: non-ideal spring behavior of the beams, stiction, and the effects of the higher modes of vibration.

Conclusion

We have presented a comparison between a simple model of a vibrating system and a complicated test fixture. Analysis of the model reveals that by carefully picking the type and speed of motion you can reduce the amount of residual vibration from a move without using a complicated controller. In particular, if the move time is short compared to the natural frequency of the system, then a simple ramp input behaves best. If the move time is on the order of the natural frequency of the system or longer, then residual vibration can be minimized by setting the time between the beginning of the acceleration and the beginning of the deceleration equal to an integral number of cycles of the system.

The theoretical results have been verified with the Flexbot. To demonstrate the complex nature of the robot, we have included maps of the natural frequencies of vibration of the Flexbot throughout its workspace. The theoretical model was compared against a series of standard moves

which showed that even though the dynamic behavior of the robot is complicated, it still behaves approximately like the simple model. In particular, we can use the theoretical model to design commands that excite a minimal amount of vibration.

We have continued to experiment with the Flexbot, comparing ramp and acceleration moves against more sophisticated control strategies, as well as experiments with motions involving changes in the vibrational frequencies and experiments in cartesian motion. For a complete description of the Flexbot and the experiments performed, refer to [6].

Acknowledgement

This report describes work done at the Artificial Intelligence Laboratory of the Massachusetts Institute of Technology. This material is based upon work supported under a National Science Foundation Graduate Fellowship. Funding for the work was provided in part by the Office of Naval Research under University Research Initiative contract N00014-86-K-0685 and in part by the Charles Stark Draper Laboratory, grants #DL-B-285399 and #CSDL-5678.

References

- [1] Alberts, T.F., Hastings, G.G., Book, W.J., and Dickerson, S.L., "Experiments in Optimal Control of a Flexible Arm with Passive Damping", *Fifth VPIISSU/ATAA Symposium on the Dynamics and Control of Large Structures*, 1985.
- [2] Bayo, E., "Computed Torque for the Position Control of Open Chain Flexible Robots", *IEEE International Conference on Robotics and Automation*, April 25-29, 1988.
- [3] Cannon, Jr., R.H. and Schmitz, E., "Initial Experiments on the End-Point Control of a Flexible One-Link Robot", *The International Journal of Robotics Research*, Vol. 3, No. 3, Fall 1984.
- [4] Christian, J.-P., "SECAFLEX: An Experimental Set-up for the Study of Active Control of Flexible Structures", *CERT/DERA*, 1989.
- [5] Christian, A.D. and Seering, W.P., "Design Considerations for an Earth Based Flexible Robotic System", *IEEE International Conference on Robotics and Automation*, May 14-19, 1989.
- [6] Christian, A.D., Technical Report #1153: *Design and Implementation of a Flexible Robot*, MIT Artificial Intelligence Lab, 1989.
- [7] Daniel, R.W., Irving, M.A., Fraser, A.B. and Lambert, M., "The Control of Compliant Manipulator Arms", *4th International Symposium on Robotics Research*, MIT Press, 1987.
- [8] Hollars, M.G. and Cannon, Jr., R.H., "Initial Experiments on the End-Point Control of a Two Link Manipulator with Flexible Tendons", *ASME Winter Annual Meeting*, November 19, 1985.
- [9] Pfeiffer, F. and Gubler, H., "A Multistage Approach to the Dynamics and Control of Elastic Robots", *IEEE International Conference on Robotics and Automation*, April 25-29, 1988.
- [10] Schmitz, E., "Modeling and Control of a Planar Manipulator with an Elastic Forearm", *IEEE International Conference on Robotics and Automation*, May 14-19, 1989.